1
2 **Porin-mediated small-molecule traffic across the outer membrane of Gram-**
3 **negative bacteria**
4

5 Julia Vergalli[1,#], Igor Bodrenko[2,#], Muriel Masi[1,#,§], Lucile Moynié[3,4], Silvia Acosta-
6 Gutiérrez[2], James H. Naismith[3,4], Anne Davin-Regli[1], Matteo Ceccarelli[2], Bert van
7 den Berg[5], Mathias Winterhalter[6], Jean-Marie Pagès[1,*]
8
9

10 [1] Aix Marseille Univ, INSERM, SSA, IRBA, MCT, Marseille 13005, France
11 [2] Department of Physics, University of Cagliari, and CNR/IOM, Cittadella Universitaria
12   di Monserrato, 09042 Monserrato (CA).
13 [3] Division of Structural Biology, Nuffield Department of Medicine, 7 Roosevelt Drive,
14   Oxford, OX3 7BN, United Kingdom.
15 [4] Rosalind Franklin Insitute, Rutherford Laboratory, Didcot, OX11 0FA, United
16   Kingdom
17 [5] Institute for Cell and Molecular Biosciences, The Medical School, Newcastle
18   University, Newcastle upon Tyne NE2 4HH, United Kingdom.
19 [6] Department of Life Sciences and Chemistry, Jacobs University Bremen, 28719
20   Bremen, Germany.
21

22
23 # These authors contributed equally to this work
24 § Present address: Institut de Biologie Intégrative de la Cellule (I2BC), Université
25 Paris Sud, Orsay cedex, France.
26
27
28 * Corresponding author
29 Jean-Marie Pagès,
30 UMR_MD1, INSERM-1261, Membranes et Cibles Thérapeutiques, Faculté de
31 Pharmacie, 27 Bd Jean Moulin, 13385 Marseille cedex05, France.
32 jean-marie.pages@univ-amu.fr
33

Abstract

Gram-negative bacteria and their complex cell envelope comprising an outer and inner membrane are an important and attractive system for studying the translocation of small molecules across biological membranes. In the outer membrane of *Enterobacteriaceae*, trimeric porins control the cellular penetration of small molecules, including nutrients and antibacterial agents. The synergistic action between relatively slow porin-mediated passive uptake across the outer membrane and active efflux transporters in the inner membrane creates a permeability barrier that re-inforces the enzymatic modification barrier, which efficiently reduces the intracellular concentrations of small molecules and contributes to the emergence of antibiotic resistance. In this review, we discuss recent advances in our understanding of the molecular and functional roles of classic porins in small molecule translocation in *Enterobacteriaceae* and consider the crucial role of porins in antibiotic resistance.

Commented [w1]: Is this specification necessary here?, in my opinion it deviates, better to put later…

Commented [JP2]: Editor request…

Introduction

Gram-negative bacteria have a complex cell envelope that comprises an outer membrane and an inner membrane, which together delineate the periplasmic space[1-3]. The inner or cytoplasmic membrane (IM) is a largely symmetrical phospholipid bilayer that is responsible for diverse physiological and metabolic functions. The outer membrane (OM) is the first line of defense, forming a physical/mechanical barrier that strongly protects the cell against external aggressive agents such as antibiotics, disinfectants, cationic peptides and bacteriocins[2-4]. The OM contains proteins that mediate the passive or active uptake of small molecules for growth and cell function[4,5].

OM proteins form β-barrels composed of 8-22 β-strands that have been characterized and classified according to their structure (monomeric or trimeric), their substrate specificity (*e.g.* specific diffusion channels for sugars like LamB) or mode of action, (*e.g.* active TonB-dependent transporters for metals and vitamins, like FhuA and BtuB, and general or classical porins for the non-specific diffusion of solutes with a molecular cutoff around 600 Da). Porins represent a substantial fraction of the total OM proteins in *Enterobacteriaceae* (> 10^5 copies/cell)[4]. *Escherichia coli* produces three major trimeric porins, namely OmpC and OmpF that exhibit selectivity for cationic molecules and PhoE with a preference to anionic molecules[4,5].

OmpF and OmpC orthologs are present in closely related *Enterobacteriaceae*, including *Enterobacter aerogenes* now termed *Klebsiella aerogenes* (Omp35 and Omp36), *Enterobacter cloacae* (OmpEc35, OmpEc36) and *K. pneumoniae* (OmpK35 and OmpK36)[4-6]. Besides their role as hydrophilic channels, porins contribute to membrane stability and participate in various physiological events of bacterial life. For example, they are major components of OM vesicles released by bacteria and can play a role during inflammation and response of the host immune system[7-11]. They can also be involved in cell-cell contacts as reported for the *Providencia stuartii* OmpPst1[12]. In addition, OmpF is required during the entry of colicins and the cell-surface exposed loops of porins are involved in the colicin E3 translocation across the OM[13].

β-lactams and fluoroquinolones are the two prominent classes of antibiotics used in clinics for treating infections caused by Gram-negative pathogens[2,3,6]. Importantly,

84 porins represent the preferred route for the entry of β-lactams, including
85 cephalosporins, penicillins and carbapenems[14-16]. The clinical relevance of
86 membrane-associated mechanisms (MAMs) of resistance (*i.e.* porin defects and/or
87 overexpression of multidrug efflux pumps[5]) has been well established for these
88 antibiotics. The Influx and Efflux rates control the internal concentration of antibiotics
89 and represent the first lane (mechanical barrier) protecting the bacterial cells against
90 therapeutic treatment[1-3,6]. Consequently, studies on bacterial porins are receiving a
91 renewed interest due to their key role in the bacterial susceptibility towards clinically
92 used antibiotics. In combination with the expression of antibiotic-modifying enzymes
93 expressed in the periplasm (e.g. β-lactamases), porins play a key role in β-lactam
94 resistance[4,17].
95
96 In this review, we discuss recent advances in our understanding of the molecular and
97 functional roles of classic porins in antibiotic translocation in *Enterobacteriaceae*. We
98 explore structural aspects and the insights gained into permeation and the pore
99 translocation process, the regulation of porin expression as well as the role of porins
100 in the emergence of antibiotic susceptibility.
101
102
103
104 **Enterobacterial general porins**

105 ***Structural aspects***
106 The crystal structures of a general porin from *Rhodobacter capsulatus*[18], the OmpF
107 and PhoE porins from *E. coli*[19] and other *E. coli* OmpF structures including
108 mutants[20,21] were the first to be solved. Only a limited number of other enterobacterial
109 porin structures have been reported, *i.e. E. coli* OmpC, *K. pneumoniae* OmpK36 and
110 *Salmonella typhi* OmpF[22-24]. The lack of data has hindered attempts to relate
111 structure to function. Recently, the structures of two porins from *P. stuartii* as well as
112 the structures of the OmpF and OmpC orthologs of *K. pneumoniae*, *E. aerogenes*
113 and *E. cloacae* have been reported[12,25,26]. Another recent study reported that *E. coli*
114 OmpF, OmpC and *K. pneumoniae* OmpK36 form complexes with MlaA, the
115 phospholipid translocation channel component of the Mla system. The complex is
116 critical to maintain the lipid asymmetry of the OM[27]. The X-ray crystal structures of *K.*

117 *pneumoniae* MlaA with OmpK36 and *E. coli* OmpF showed that MlaA is a pore-
118 containing, α-helical OM protein that selectively removes phospholipids from the
119 outer OM leaflet[28]. As formation of a complex with MlaA does not seem to alter the
120 structure of the porins, it seems likely that the porins function as scaffolds for MlaA
121 and that their function is not affected by the bound lipoprotein. In this review we focus
122 on porins as isolated molecules[28].

123

124 Porins are often organised as trimers, with inter-monomer contacts provided by the
125 hydrophobic surfaces of the barrels and by extracellular loop L2, which latches into a
126 groove of a neighbouring monomer and makes a number of polar interactions
127 **(FIGURE 1).** The trimer entity itself seems to have no clear function as no strong
128 evidence has suggested that cooperativity exists within the trimer, *i.e.* the porin
129 monomers likely function as independent subunits. The trimeric arrangement may
130 simply confer additional stability. Viewed as a cross-section perpendicular to the
131 membrane, the channels have an hourglass shape, with the narrowest part named
132 "eyelet" or constriction region (CR, see **FIGURE 1c, e**). For *E. coli* OmpF and OmpC,
133 the CR has a roughly circular shape with diameters of 6.5-7 Å and 5.5-6 Å
134 respectively. The CR is the consequence of the presence of the ~35 residue-long
135 extracellular loop L3, which folds inwards to generate a narrow pore (**FIGURE 1**);
136 without it, the resulting huge pore of ~15 x 23 Å would severely compromise OM
137 impermeability. Another, crucial consequence of the L3 loop is the generation of a
138 strong (transverse) electric field across the CR, resulting from a row of positively
139 charged residues on the barrel wall (K16, R37, R74 and R124 in *E. coli* OmpC) that
140 lie opposite negatively charged residues (Asp105 and Glu109 in OmpC) and
141 backbone carbonyl groups on L3 that point into the CR (**FIGURE 2**). This electric field
142 has two important but distinct roles in controlling transport through the OM. First, it
143 orients water molecules inside the pore, making it energetically unfavourable for
144 hydrophobic small molecules to displace them and thus permeate through the CR.
145 Second, the electric field has also direct consequences for the permeation of polar
146 small molecules, as its shape and size have been shown to determine the efficiency
147 with which molecules can pass the CR. The polarity in the CR also results in different
148 permeation paths for simple anions relative to cations[29]. Although a large number of
149 basic residues exposed into the eyelet region, both OmpF and OmpC with their
150 orthologs are slightly cation selective, with a higher selectivity for OmpC-like porins

151 [REF Acosta ACS-ID 2018]. In addition, the smaller size of OmpC-like porins
152 determines a lower conductivity of ions with respect to OmpF-like porins. Early study
153 showed that point mutations can alter in both direction permeability [REF Misra, R.,
154 and Benson, S.A. (1988) Isolation and characterization of OmpC porin mutants with
155 altered pore properties. J. Bacteriol. 170: 528-533]. With the support of high
156 resolution structures and modelling, the sSubtle perturbation of the electric field by
157 mutation of residues was shown to be partly behind the development of clinical
158 resistance[30].

159

160 **_Substrate specificity_**
161 An important issue is the substrate specificity of general porins and the question
162 whether these channels have _bona fide_ binding sites for their substrates[31]. Early
163 electrophysiological studies described transient current blockages of _E. coli_ OmpF in
164 the presence of various small molecules including antibiotics[32] suggesting weak
165 binding sites in the vicinity of the CR. Obtaining structural confirmation for any
166 potential binding sites has proven challenging, but the co-crystal structures for three
167 antibiotics (ampicillin, carbenicillin and ertapenem) and _E. coli_ OmpF were reported[33].
168 Importantly, the antibiotics occupy very different positions with ertapenem bound in
169 the extracellular vestibule, ampicillin on the extracellular side of the CR and
170 carbenicillin in the periplasmic vestibule. Notably, none of the compounds are bound
171 in the CR, and only for ampicillin did the occupation of the observed binding site
172 result in current blockages by computational electrophysiology[33]. Moreover, the
173 structures were obtained with extremely high concentrations of antibiotics (1-2 M),
174 _i.e._ at least four orders of magnitude higher than would likely be encountered _in vivo_.
175 However, small decreases (up to 4-fold) in MIC values for _E. coli_ were observed for
176 selected single mutations of polar or charged residues in the ampicillin and
177 carbenicillin binding sites. While these results suggest that disruption of a possible
178 antibiotic binding site _increases_ susceptibility, the very different locations of the sites
179 raise some questions. An alternative and plausible explanation would be that the
180 observed effects on antibiotic susceptibility are caused by local changes in the
181 electrostatics of the channel, which would echo the observation that subtle changes
182 in electrostatic properties can influence antibiotic permeation[30]. Thus, in terms of
183 specificity, there is a clear difference between general porins and truly substrate-
184 specific channels such as LamB and Tsx, where mM concentrations or lower are

Commented [MC3]: to reply to referee-1

185 sufficient to occupy substrate binding sites in crystal structures[34,35]. Nevertheless,
186 mounting recent evidence clearly suggest that general porins are in part selective
187 and allow passage of some compounds much more readily than others. Relating
188 such preferential permeability to protein sequence would be powerful in designing
189 antibiotics. A systematic study on the permeation of a series of antibiotics mediated
190 by four OmpF/OmpC pairs (from *E. coli*, *K. pneumoniae*, *E. aerogenes* and *E.*
191 *cloacae*) was reported recently[25]. This study showed that enterobacterial porin
192 structures are topologically identical and even in detail very similar (**FIGURE 2**).
193 However, analysis show that very subtle differences in structure lead to alteration of
194 the electric field close to and within the constriction zone and are accompanied by
195 differences in the permeation of antibiotics[25]. The new data allowed the development
196 of a new quantitive scoring function for antibiotics permeation that is in broad
197 agreement with *in vitro* permeation data. Thus, given a structure, it is now possible to
198 predict what molecules are favored or disfavored in terms of permeation. Another
199 recent study reported a set of more qualitative permeation rules, and used these to
200 convert, via addition of an amine group, a narrow-spectrum compound (6-DNM) into
201 a compound (6-DNM-NH_3) that efficiently permeated *E. coli* as evidenced by 2 to 64-
202 fold lower MIC values[36]. Interestingly, the data also showed lower MIC values for 6-
203 DNM-NH_3 in *Pseudomonas aeruginosa* and *Acinetobacter baumannii*, despite the
204 fact that these non-enteric pathogens lack general porins and instead possess
205 substrate-specific channels. This in turn suggests that the structural properties that
206 govern small-molecule permeation through *E. coli* porins may be, at least to some
207 extent, broadly conserved in Gram-negative bacteria. While further work is certainly
208 required, these studies provide clear hope for the design of more efficiently
209 permeating antibiotics.

210
211
212

213 **Porin-mediated transport**

214 ***Experimental tools to characterize permeation across porins***
215 Early approaches to quantify small molecule uptake across Gram-negative cell
216 envelopes revealed a correlation between the presence of porins and selective
217 uptake across the outer cell wall. Isolation of porins and reconstitution into artificial

bilayers allowed conductance measurements to characterize single channels. In addition to ion selectivity, a statistical analysis of the conductance distribution suggested pore sizes of around one nanometer, close to that revealed by high resolution X-ray structures a few years later[19].

A complementary permeation technique was the so-called liposome swelling assay, whereby kinetic information on the uptake through the porins was obtained[5]. Another method used to characterise indirectly the influx is to measure the endogenous periplasmic β-lactamase activity. Following the degradation product of antibiotics optically allowed to estimate their diffusion rate across OmpK35 and OmpK36 porin and showed a remarkably high permeability toward lipophilic (benzylpenicillin) and large (cefepime) compounds[37]. These results suggest a larger and more permeable channel for OmpK35 and OmpK36 than their *E. coli* homologs OmpF and OmpC explaining why drug resistance in *K. pneumoniae* caused by the loss of porins is often reported in clinical isolates[37]. The recent technical breakthrough lead to ultrasensitive mass spectrometers allowing now whole cell accumulation assays. However, the sensitivity is not yet at single bacteria level and the crucial part in using the mass spectrometry method is to separate those molecules attached to the LPS outside of the cell from those that have truly penetrated[36,38-44]. For example, a study[45] revealed differences in ciprofloxacin accumulation between strains with efflux pumps compared to those with deactivated ones. Direct information on the accumulation of antibiotics in single bacterial cells[45-47] can be obtained using deep UV autofluorescence microscopy.

A different method to characterize channel transport is to use the ion current as a probe for transport. Earlier work introduced the ion-current fluctuation to reveal on and off rates of sugar into the sugar-specific channel LamB[48,49].This analysis requires a strong binding of the molecule inside the channel and once inside the binding site the molecule must sufficiently block the ion current[50-54]. Transferring this approach to other small molecules with low or no affinity to the channel is not straightforward. (see BOX 1 for more details). A different approach involves the use of an unbalanced charge accumulation[55,56]. Creating a concentration gradient between both sides of the channel induces a concentration-driven flux (**BOX 2**). Unequal diffusion of the

251 charged compound versus the counterion created the so-called diffusion potential
252 that can be easily recorded.
253

254 ***The translocation process at atomic level***
255 Predicting the number of molecules per second that translocate through porins
256 (molecular flux) is a computationally and experimentally challenging task[57]. The

Commented [MC4]: Please cite again Ref Kullmann Biophys. J. 2002

257 molecular flux is ultimately governed by the statistically averaged molecular
258 interactions, or the free energy, of the molecule with the pore and the solvent water[58].
259 The first MD simulation of OmpF in a fully solvated symmetric bilayer revealed the
260 alignment of water molecules at the CR of the pore[59], highlighting the already
261 hypothesized existence of a strong electric field, transversal to the diffusion axis.
262 Later, MD and Brownian dynamics simulations have shown two distinct paths for
263 diffusion of anions and cations[60]. OmpF selectivity was also studied by means of
264 macroscopic electrodiffusion models and the combination of molecular dynamics with
265 electrophysiology experiments has started to elucidate the role of temperature and
266 pH in ion-selectivity for both OmpF and OmpC porins from *E. coli*[61,62]. This type of
267 work emphasises the notion that the permeating ions interact with the wall of the
268 channel and that ion movement does not follow simple diffusion. Further, for the
269 permeation of larger molecules such as antibiotics it is expected that the interaction
270 with the surface of the channel is likely the rate-limiting factor. Cavity solvation
271 energetics calculations in OmpC were used to infer compound permeability from its
272 ability to replace favorable water molecules prior to ligand association[63].
273 The first attempts to calculate the free energy interaction of the antibiotic with the
274 pore surface applying advanced sampling techniques, such as metadynamics,
275 allowed the identification of barriers and affinity sites close to the CR[64]. These studies
276 when combined with electrophysiology data suggested that favourable interactions in
277 the CR correlate with enhanced diffusion through OmpF, introducing the binding site
278 concept in the permeation problem[64], supported by studies on site-directed
279 mutagenesis of key residues in the CR affecting β-lactam influx and susceptibility[5,65].
280 However, as pointed out, crystallographic studies showed that there is not a unique
281 binding site inside OmpF[33], and in the case of the zwitterionic ampicillin, its binding
282 mode in the co-complex was not located in the CR but above it, in the so-called pre-
283 orientation region[66].
284

The recent introduction of Graphic Processor Unit (GPU) for scientific computing allowed extending the calculation of the antibiotic-pore interactions to the entire pore length, opening the way to the introduction of the free energy landscape model to rationalize the translocation process (see **BOX 2**). The simulations enabled elucidation of the role of the main features of porin archictecture on the diffusion of dipolar molecules (**FIGURE 3**), showing how those molecules align their electric dipole moment with the internal electrostatic field in the pore[66,67], similar to water. Moreover, the quantification of the electric field of porins, based on the analysis of water polarization in all-atom simulations, confirmed that its largest component is directed transversally to the axis of diffusion and is modulated by environmental factors such as pH and salt concentrations[68]. The internal electric field of porins is thus a key pore property that fine-tunes its selectivity filter and explains also why the permeation rate of penicillins in OmpF decreases and becomes comparable to that in OmpC at high salt concentrations, as observed experimentally[69]. ~~Subtle differences in electrostatics, due to mutations of charged OmpC residues in a series of clinical isolates, explain the different susceptibility of the mutated strains[30].~~

The successful combination of electrophysiology, enhanced sampling techniques and an improved excess noise statistical analysis made it possible to quantify the kinetic parameters such as the residence time of molecules inside the pore[70] even well below the resolution time of the apparatus[71,72]. Further, the permeation of norfloxacin through OmpF demonstrated the existence of the transversal electric field and its effect on the transport of dipolar molecules[73]. Finally, the permeation of three β-lactamase inhibitors (avibactam, sulbactam and tazobactam) through OmpF and OmpC orthologs from four enterobacterial species was recently characterised using the charge unbalance method (**BOX 2**). The experimental quantification of the permeation rate~~flux~~ of molecules allowed to test and verify the free energy landscape model presented in Fig. 3~~(descripted below ? or in Figure3?)~~: the main barrier in the CR is caused by the pore's size reduction and for ions is low and broad whereas for the β-lactam inhibitors is slightly higher but substantially narrower[56] because of dipolar interactions with the electric field.

Molecular parameters controlling permeation

Our knowledge about small molecule permeation in Gram-negative bacteria mostly came from the post-analyses of molecular properties of effective antibacterial

agents[74-76], which have suggested polarity and molecular weight as key factors for determining permeation[75]. It is interesting to note how in the last two generation of cephalosporins all molecules are zwitterionic, with an additional positive group in the scaffold[77]. Only recent studies confirmed the importance of having a positive charge in the scaffold for a better penetration through cation-selective porins such as OmpF/OmpC[73]. In particular a systematic study on diverse molecular scaffolds (>150 molecules), not necessarily with antinfective property, showed that the addition of an amine group can enhance accumulation in *E. coli*[36]. The new high-resolution X-ray structures of OmpF/OmpC orthologs from *Enterobacteriaceae*[25], together with those obtained from *E. coli* clinical strains[30], allowed a thorough computational investigation, which revealed the common filtering mechanism of general porins (**FIGURE 3**). From the systematic analysis of permeability data on nine clinically relevant antibiotics through the eight enterobacterial porins, it was shown that the main energetic barrier located in the CR along the diffusion axis ultimately regulates the molecular permeability. By incorporating this molecular mechanism in a scoring function (or a supervised machine learning algorithm), it was possible to predict molecular permeability through porins. The scoring function is based on two energetic terms, $F_{steric} + F_{electrostatic}$, which depend on the physico-chemical parameters of molecules, pores and solvents. It also suggests the following three useful conclusions about the molecular permeability through porins. First, the permeability is the ability to overcome a barrier, and hence, molecules need to be designed for their ability to pass the CR rather than to bind to the pore. Second, the parameters describing the molecules and the pores in the scoring function are obtained from statistical averages of physical observables along molecular dynamics simulations. Importantly, the steric term depends not only on the size of each molecule and on that of the pore but also on their fluctuations[78]. Thus, in many cases the permeation is only possible because the molecules and pores change their size due to spontaneous fluctuations induced by temperature. Third, although the size reduction of the pore in the CR accounts for the biggest part of the barrier (F_{steric}), the electrostatic interaction ultimately shapes the barrier, either decreasing it or increasing it. Molecules with similar sizes can have very different permeabilities due to the electrostatic interactions with the pore. The reason is that the free energy barrier appears in the expression of permeability within an exponential function (**Figure 3**)[58]. Therefore, fine-tuning of charge distribution and thus the charge and

Commented [MC6]: Ok the ref 77 here

Commented [VJ7]: Ref 77 here, is it ok?

353 dipole moment of compounds should be considered when optimizing molecules for
354 optimal permeability through porins[66].

355

356

357

Regulation of porin expression

359 The regulation of classical porin expression in *Enterobacteriaceae* is complex
360 (**SupplementaryInformation Figure**). Classical porin genes are transcribed as
361 monocistronic mRNAs, which does not exclude co-regulation with other genes in
362 their vicinity. Regulation of porin expression involves multiple genetic effectors and
363 regulatory cascades[79-85]. These include transcriptional regulators of the XylS/AraC
364 family, which are responsible for chemical stress responses; two-component systems
365 (TCS), in which a sensor kinase in the IM detects a signal that is transmitted to a
366 cytoplasmic regulator; and extracytoplasmic function (ECF) sigma factors, which can
367 redirect some or all of the RNA polymerase to activate transcription. In particular,
368 alternative sigma factor σ^E and TCS CpxAR contribute to the major envelope stress
369 response (ESRs) pathways by detecting envelope alterations and modulating gene
370 expression to limit the stress impact[79,81,85]. These ESRs have a common regulon and
371 interconnections that can regulate similar gene expression in response to different
372 stress. Importantly, both σ^E and Cpx regulate and are regulated by small regulatory
373 RNAs (sRNAs) involved in the post-transcriptional response to envelope stress.

374

375 Due to their different channel properties and the role these play in OM permeability,
376 the expression of OmpF and OmpC is tightly regulated by several factors (for recent
377 reviews see[6,16,65,81]). Osmolarity is probably the best-understood environmental
378 signal that modulates OmpF and OmpC expression via the EnvZ/OmpR TCS
379 (**SupplementaryInformation Figure**)[65]. After activation by external signal, the
380 phosphoryl group of autophosphorylated EnvZ is transferred to OmpR. Thus,
381 phosphorylated OmpR (OmpR~P) acts as a transcription factor that differentially
382 modulates the *ompF* and *ompC* expression. The *ompF* gene is transcribed at low
383 osmolarity when the OmpR~P level is low and binds only the high-affinity binding
384 sites present on *ompF*. Conversely, when the concentration of OmpR~P increases
385 due to high osmolarity, OmpR~P occupies all binding sites available on *ompF* and

386 *ompC* and this sequential binding triggers the differential expression of the porin
387 genes, *e.g.* increased transcription of *ompC* and repression of *ompF.*

388 Recent advances in RNA-based techniques[86,87] have increased our knowledge about
389 the repertoire of bacterial sRNAs and their impact on OMP expression[88-90].
390 Importantly, sRNAs govern gene expression and allow a fast and efficient adjustment
391 to different growth conditions. OmpF is post-transcriptionally repressed by the sRNA
392 MicF. The control of the MicF sRNA expression depends on multiple signals and
393 regulatory pathways[91]. This 93-nucleotide (nt) RNA is divergent to the *ompC* gene
394 and acts by a direct base-pairing to a region that encompasses the ribosome binding
395 site (RBS) and the start codon of the *ompF* mRNA, thus preventing the initiation of
396 translation and favoring degradation[92-94]. Moreover, the positive regulation also
397 includes EnvZ/OmpR in high osmolarity conditions, SoxS in response to oxidative
398 stress and MarA in response to antibiotic stress[95,96]. More recently, a 109-nt MicC
399 sRNA has been identified and is able to repress OmpC by a direct base-pairing to a
400 5' untranslated region of the *ompC* mRNA[97]. Noteworthy, MicC is transcribed
401 opposite to the *ompN* gene that encodes a quiescent porin and it has recently been
402 reported that *ompN* and *micC* are submitted to complex regulation upon exposure to
403 β-lactam antibiotics[98]. This is consistent with *ompN-micC* and *ompC-micF* sharing a
404 similar genetic organization and that *ompC* and *micF* are co-induced under specific
405 conditions (i. e. high osmolarity via EnvZ/OmpR).

406

407 The contribution of XylS/AraC transcriptional regulators in controlling envelope
408 permeabilty has been known for some time. These include MarA that is the key
409 transcriptional regulator encoded by the *marRAB* operon, RamA, SoxS and Rob,
410 which synergistically contribute to decrease the antibiotic accumulation inside the
411 bacterial cell via downregulation of porin genes and increase of antibiotic efflux via
412 upregulation of multridrug efflux pumps such as AcrAB. MarRAB plays a central role
413 in the enterobacterial response to external agents including antibiotics, detergents,
414 disinfectants and preservatives[6,99,100]. In particular, MarA can inhibit porin expression
415 - directly at the transcriptional level, through binding to a conserved Marbox in the
416 promoter region of porin gene, and - indirectly at the post-transcriptional level by
417 activating MicF (**SupplementaryInformation Figure**). Various point mutations
418 and/or deletions in *marA* and *marR* have been reported in several clinical strains and
419 contribute to the emergence of clinical MDR phenotypes[65].

An additional regulator, RamA-RamR has been identified in *Enterobacter spp.*, *Klebsiella spp.*, *Salmonella spp.* but is absent in *Escherichia coli*[6,16,99,100]. RamA is able to directly enhance MarA transcription and a conserved marbox is detected in the two promoters of these genes. RamA is also able to control the expression of porins in *Enterobacter spp.* and *Klebsiella spp.*[65,100,101].

Porins and antibiotic susceptibility

Porin expression (TABLE 1)

Several reports describe an alteration of porin expression (OmpF and OmpC) in *E. coli* clinical strains during antibiotherapy[5]. A recent study describes a point mutation in the OmpR regulator that induces a conformational change involved in the repression of porin gene expression and thus in carbapenem resistance[102]. Moreover, in various collections of carbapenem non-susceptible *Enterobacteriaceae,* porin expression correlates with the level of carbapenem resistance[103]. This porin-susceptibility relationship seems to be associated with the characteristics of the porin channel, (OmpC type versus OmpF type), as recently discussed for β-lactam class compounds[6,25,67]. In *P. stuartii*, a defect of OmpPst1 expression or the presence of mutations in the corresponding gene have been described in resistant clinical strains[104,105]. These mutations are located in extracellular loops, which might be involved in trimer flexibility and may contribute to the active conformation of the porin[12,105]. Regarding *K. pneumoniae*, *E. cloacae* and *E. aerogenes*, the development of drug resistance is often found associated with a reduced level of porin expression or the mutational loss of its major porins[103,106-109]. Similarly, *Salmonella enterica* serovar Typhimurium developed carbapenem resistance during ertapenem treatment due to an OmpC deficiency[110].

Drug resistance in *Enterobacteriaceae* is mostly caused by lack of or reduced expression of the major porins combined with various β-lactamases and efflux pumps expressions: these mechanisms cooperate to strongly decrease the level of active antibiotic in the periplasm[103,111-115]. The efficiency of efflux pumps and β-lactamases is strongly increased because in porin-deficient cells the concentrations of antibiotics in periplasm are below the saturation levels of enzymes and transporters (BOX 3). Consequently, porin deficiency has been reported in clinical isolates of extended-

15

spectrum β-lactamases (ESBL)-producing *Enterobacteriaceae* resistant to other compounds, such as quinolones[116].

Importantly, a whole genome sequencing study combined with phenotypic and biochemical characterizations has demonstrated the sequential emergence of target mutations associated with alteration of porin expression in *E. aerogenes* isolates collected during antibiotic treatments of two patients[107].

The sequential replacement of expressed porin (OmpF substituted by OmpC family expression) results in reduced influx and correlates with the resistance phenotype observed in *Enterobacteriaceae* isolates: susceptible isolates express both major porins, low level / intermediate resistant isolates exhibit one truncated porin, and the loss of both major porins leads to the highest level of resistance with a complete impermeability to β-lactams[6,65,107,111,117-120]. It was also reported that the expression of a truncated OmpK36 during carbapenem treatment provided a wider spectrum of resistance[121,122]. Other mutations in *ompK35* and *ompK36* have been reported as the most likely contributor to ceftazidime-avibactam resistance in several *K. pneumoniae* strains[123-126]. The reported mutations directly affect the porin expression or, due to their location in the OmpK36 internal loop, affect the activity of imipenem-relebactam or meropenem-varbobactam combinations[127,128].

Commented [JP8]: this is clinical observation

***Mutation in the porin CR* (TABLE 1)**

Enterobacteriaceae isolates express variants of OmpC orthologs resulting from the substitution or insertion of one or two amino acids in loop L3 at or near the CR of the porin channel (**FIGURE 1**). Gly->Asp substitution located in the PEFXGD motif of the L3 loop[5], was detected in β-lactam resistant isolates of *E. aerogenes* and *K. pneumoniae*[129-131]. An OmpK36 variant, exhibiting two additional amino acids (Asp137 and Thr138) in the loop, shows both ertapenem resistance and a reduced meropenem susceptibility[132]. The concerved PEFXGD motif forms a turn in the L3 loop and so contribute to the formation of the CR. Interestingly, the mutation Gly->Asp in this domain is also involved in ceftazidime-varbobactam resistance[128]. Several other studies have reported a similar variant of OmpK36 with insertion of either Asp-Gly or Gly-Asp in L3, conferring a resistance to carbapenem[114,133-136]. OmpC mutants in *E. coli* clinical strains present diverse mutations in the channel constriction that perturb the transverse electric field in CR without reducing its size, thus trapping the drug in an orientation unfavorable for permeation[30,67].

Consequently, the translocation efficacy of antibiotic across the channel is decreased, providing reduced periplasmic accumulation and a decrease in β-lactam susceptibilities, independent of porin expression levels[5]. Importantly, this reduced internal amount is associated with an induction of ß-lactamase expression[128].

Alternative porins

Enterobacteriaceae are able to express alternative porins to balance the loss of classical porins[5,123]. Overexpression of LamB has been reported in resistant isolates of *E. aerogenes* and *K. pneumoniae* yielding to a reduced antibiotic susceptibility while preserving bacterial fitness[5,65,137]. A correlation between phosphoporin PhoE expression and carbapenem susceptibility has been reported in clinical isolates of *K. pneumoniae* devoid of OmpK35 and OmpK36. The first isolate displayed carbapenem resistance, the second was susceptible to all carbapenems due to its constitutive expression of PhoE, and the third isolate was resistant to ertapenem and cefoxitin but susceptible to imipenem since it expressed PhoE at a low level[138]. No fitness alteration for the two PhoE expressing isolates was observed. Downregulation of PhoE has also been previously observed in carbapenem resistant *K. pneumoniae* isolates[139]. Interestingly the expression of OmpK26 porin, which usually transports acidic oligosaccharides, confers carbapenem low susceptibility in the absence of OmpK36 in a *K. pneumoniae* isolate[137]. However, this OmpK26 expression does not restore the fitness due to OmpK36 loss[137]. *K. pneumoniae* can also induce the expression of the quiescent porin OmpK37 (the ortholog of *E. coli* OmpN) to maintain its fitness[140] but this porin seems to play only a minor role in β-lactam resistance[111,139-141].

Concluding remarks

The regulation of porin expression involves several modes of regulation. In addition, the final assembly as functional trimers into the OM is tightly controlled by the BAM machinery but also requires LPS binding[26,142-144]. These complex and partly redundant systems efficiently control the production of porins, which represent a prominent part of the OM protein landscape and are directly involved in OM permeability. The regulation systems are also responsible for a rapid adaptation

522 following external stresses such as antibiotics, chemicals, and colicins[1,6]. It should be
523 stressed that only few studies have studied a possible role of MicF and MicC in the
524 alteration of OM permeability in resistant strains[145-147]. To define the contribution of
525 sRNA post-transcriptional silencing of porin genes in the regulation of porins, it
526 seems important to investigate this aspect in addition to other regulators (MarA,
527 RamA, etc) in clinical isolates during antibiotic treatment. It is also important to
528 consider all flux across bacterial membranes (Influx and Efflux) as a continuum that
529 controls the internal concentration of drugs via a coordinated regulation of
530 transporter/porin expression.

531

532 The internal conserved architecture of the channel inside the CR with its distribution
533 of negative and positive charges and resulting electrostatic field is the strategic check
534 point controling the entrance of small polar compounds. In this key region, several
535 specific mutations can alter the channel properties and increase or decrease the
536 influx rate of molecules across the OM (for recent reviews see [6,65]).
537 Since porin channels represent an Achilles heel in the membrane barrier that
538 protects the bacterial cell against toxic external compounds, it is not surprizing that
539 the loss of porin has often been reported in resistant clinical isolates. While allowing
540 the bacteria to grow during antibiotherapy, the deficiency of major porins has a
541 significant effect on the fitness and virulence of these resistant isolates.
542 Consequently, clinical isolates encoding altered but still functional porins or alternate
543 porins might have an advantage over isolates with non-functional porins. This
544 strategy generates a minimal fitness cost for the bacterial cell while at the same time
545 decreasing antibiotic susceptibility, which would contribute to the selection and the
546 successful spread of resistant phenotype isolates.

547

548 Recent technical advances allow measuring the rate of compound accumulation
549 inside individual bacterial cells and the translocation through reconstituted porin
550 channels *in vitro*, the simulation of the journey of small molecules inside the pore,
551 and the pharmacomodulation of new pore-permeating compounds. These advances
552 will undoubtedly help us to understand the translocation of drugs across bacterial
553 membranes and will enable the design-improved molecules with better penetration
554 and accumulation within Gram-negative bacteria.

555

556

557

558

Acknowledgments

573

574

575

REFERENCES

1. Nikaido, H. Outer membrane barrier as a mechanism of antimicrobial resistance. *Antimicrob Agents Chemother* **33**, 1831–1836 (1989).

2. Zgurskaya, H. I., Löpez, C. A. & Gnanakaran, S. Permeability barrier of Gram-negative cell envelopes and approaches to bypass it. *ACS Infect Dis* **1**, 512–522 (2015).

3. Hancock, R. E. W. The bacterial outer membrane as a drug barrier. *Trends in Microbiology* **5**, 37–42 (1997).

4. Nikaido, H. Molecular basis of bacterial outer membrane permeability revisited. *Microbiol Mol Biol Rev* **67**, 593–656 (2003).

5. Pagès, J.-M., James, C. E. & Winterhalter, M. The porin and the permeating antibiotic: a selective diffusion barrier in Gram-negative bacteria. *Nat Rev Micro* **6**, 893–903 (2008).

6. Masi, M., Réfrégiers, M., Pos, K. M. & Pagès, J.-M. Mechanisms of envelope permeability and antibiotic influx and efflux in Gram-negative bacteria. *Nature Microbiology* **2**, 17001 (2017).

7. Yan, J. J., Wang, M. C., Zheng, P. X., Tsai, L. H. & Wu, J. J. Associations of the major international high-risk resistant clones and virulent clones with specific *ompK36* allele groups in *Klebsiella pneumoniae* in Taiwan. *New Microbes New Infect* **5**, 1–4 (2015).

8. Galdiero, S. *et al.* Microbe-host interactions: Structure and role of Gram-negative bacterial porins. *Curr Protein Pept Sci* **13**, 843–854 (2012).

9. Liu, Y.-F. *et al.* Loss of outer membrane protein C in *Escherichia coli* contributes to both antibiotic resistance and escaping antibody-dependent bactericidal activity. *Infect Immun* **80**, 1815–1822 (2012).

10. Salerno-Gonçalves, R. *et al.* Use of a novel antigen expressing system to study the *Salmonella enterica* serovar Typhi protein recognition by T cells. *PLoS Negl Trop Dis* **11**, (2017).

11. Pérez-Toledo, M. *et al. Salmonella* Typhi porins OmpC and OmpF are potent adjuvants for T-dependent and T-independent antigens. *Front Immunol* **8**, (2017).

607   12. El-Khatib, M. *et al.* Porin self-association enables cell-to-cell contact in
608   *Providencia stuartii* floating communities. *Proc Natl Acad Sci U S A* **115**, E2220–
609   E2228 (2018).

610   13. Cramer, W. A., Sharma, O. & Zakharov, S. D. On mechanisms of colicin import:
611   the outer membrane quandary. *Biochemical Journal* **475**, 3903–3915 (2018).

612   14. Walsh, C. *Antibiotics: actions, origins, resistance.* (American Society of
613   Microbiology, 2003). doi:10.1128/9781555817886

614   15. Bryskier. *Antimicrobial Agents: Antibacterials and Antifungals*. (American Society
615   of Microbiology, 2005). doi:10.1128/9781555815929

616   16. Dam, S., Pagès, J.-M. & Masi, M. Stress responses, outer membrane
617   permeability control and antimicrobial resistance in *Enterobacteriaceae*.
618   *Microbiology* **164**, 260–267 (2018).

619   17. Bush, K. Past and present perspectives on β-lactamases. *Antimicrobial Agents*
620   *and Chemotherapy* **62**, e01076-18 (2018).

621   18. Weiss, M. S. & Schulz, G. E. Structure of porin refined at 1.8 Å resolution. *Journal*
622   *of Molecular Biology* **227**, 493–509 (1992).

623   19. Cowan, S. W. *et al.* Crystal structures explain functional properties of two *E. coli*
624   porins. *Nature* **358**, 727 (1992).

625   20. Lou, K.-L. *et al.* Structural and functional characterization of OmpF porin mutants
626   selected for larger pore size. I. CRYSTALLOGRAPHIC ANALYSIS. *J. Biol.*
627   *Chem.* **271**, 20669–20675 (1996).

628   21. Phale, P. S. *et al.* Role of charged residues at the OmpF porin channel
629   constriction probed by mutagenesis and simulation. *Biochemistry* **40**, 6319–6325
630   (2001).

631   22. Baslé, A., Rummel, G., Storici, P., Rosenbusch, J. P. & Schirmer, T. Crystal
632   structure of osmoporin OmpC from *E. coli* at 2.0 Å. *Journal of Molecular Biology*
633   **362**, 933–942 (2006).

634   23. Dutzler, R. *et al.* Crystal structure and functional characterization of OmpK36, the
635   osmoporin of *Klebsiella pneumoniae*. *Structure* **7**, 425–434 (1999).

636   24. Balasubramaniam, D., Arockiasamy, A., Kumar, P. D., Sharma, A. &
637   Krishnaswamy, S. Asymmetric pore occupancy in crystal structure of OmpF porin
638   from *Salmonella typhi*. *Journal of Structural Biology* **178**, 233–244 (2012).

639   25. Acosta-Gutiérrez, S. *et al.* Getting drugs into Gram-negative bacteria: Rational
640   rules for permeation through general porins. *ACS Infect Dis* **4**, 1487–1498 (2018).
641   26. Arunmanee, W. *et al.* Gram-negative trimeric porins have specific LPS binding
642   sites that are essential for porin biogenesis. *PNAS* **113**, E5034–E5043 (2016).
643   27. Malinverni, J. C. & Silhavy, T. J. An ABC transport system that maintains lipid
644   asymmetry in the gram-negative outer membrane. *Proc. Natl. Acad. Sci. U.S.A.*
645   **106**, 8009–8014 (2009).
646   28. Abellón-Ruiz, J. *et al.* Structural basis for maintenance of bacterial outer
647   membrane lipid asymmetry. *Nature Microbiology* **2**, 1616 (2017).
648   29. Dhakshnamoorthy, B., Ziervogel, B. K., Blachowicz, L. & Roux, B. A structural
649   study of ion permeation in OmpF porin from anomalous X-ray diffraction and
650   molecular dynamics simulations. *J. Am. Chem. Soc.* **135**, 16561–16568 (2013).
651   30. Lou, H. *et al.* Altered antibiotic transport in OmpC mutants isolated from a series
652   of clinical strains of multi-drug resistant *E. coli. PLoS One* **6**, (2011).
653   31. Kojima, S. & Nikaido, H. Permeation rates of penicillins indicate that *Escherichia*
654   *coli* porins function principally as nonspecific channels. *PNAS* **110**, E2629–E2634
655   (2013).
656   32. Nestorovich, E. M., Danelon, C., Winterhalter, M. & Bezrukov, S. M. Designed to
657   penetrate: Time-resolved interaction of single antibiotic molecules with bacterial
658   pores. *PNAS* **99**, 9789–9794 (2002).
659   33. Ziervogel, B. K. & Roux, B. The binding of antibiotics in OmpF porin. *Structure* **21**,
660   76–87 (2013).
661   34. Dutzler, R., Wang, Y.-F., Rizkallah, P. J., Rosenbusch, J. P. & Schirmer, T.
662   Crystal structures of various maltooligosaccharides bound to maltoporin reveal a
663   specific sugar translocation pathway. *Structure* **4**, 127–134 (1996).
664   35. Ye, J. & van den Berg, B. Crystal structure of the bacterial nucleoside transporter
665   Tsx. *EMBO J* **23**, 3187–3195 (2004).
666   36. Richter, M. F. *et al.* Predictive compound accumulation rules yield a broad-
667   spectrum antibiotic. *Nature* **545**, 299–304 (2017).
668   37. Sugawara, E., Kojima, S. & Nikaido, H. *Klebsiella pneumoniae* major porins
669   OmpK35 and OmpK36 allow more efficient diffusion of β-lactams than their
670   *Escherichia coli* homologs OmpF and OmpC. *J Bacteriol* **198**, 3200–3208 (2016).

671   38. Cai, H., Rose, K., Liang, L.-H., Dunham, S. & Stover, C. Development of a liquid
672   chromatography/mass spectrometry-based drug accumulation assay in
673   *Pseudomonas aeruginosa*. *Analytical Biochemistry* **385**, 321–325 (2009).

674   39. Schumacher, A. *et al.* Intracellular accumulation of linezolid in *Escherichia coli*,
675   *Citrobacter freundii* and *Enterobacter aerogenes*: role of enhanced efflux pump
676   activity and inactivation. *J Antimicrob Chemother* **59**, 1261–1264 (2007).

677   40. Davis, T. D., Gerry, ChristopherJ. & Tan, D. S. General platform for systematic
678   quantitative evaluation of small-molecule permeability in bacteria. *ACS Chem Biol*
679   **9**, 2535–2544 (2014).

680   41. Zhou, Y. *et al.* Thinking outside the "Bug": A unique assay to measure
681   intracellular drug penetration in Gram-negative bacteria. *Anal. Chem.* **87**, 3579–
682   3584 (2015).

683   42. Iyer, R. *et al.* Evaluating LC-MS/MS to measure accumulation of compounds
684   within bacteria. *ACS Infect Dis* **4**, 1336–1345 (2018).

685   43. Six, D. A., Krucker, T. & Leeds, J. A. Advances and challenges in bacterial
686   compound accumulation assays for drug discovery. *Current Opinion in Chemical*
687   *Biology* **44**, 9–15 (2018).

688   44. Prochnow, H. *et al.* Subcellular quantification of uptake in Gram-negative
689   bacteria. *Anal. Chem.* **91**, 1863–1872 (2019).

690   45. Vergalli, J. *et al.* Fluoroquinolone structure and translocation flux across bacterial
691   membrane. *Scientific Reports* **7**, 9821 (2017).

692   46. Vergalli, J. *et al.* Spectrofluorimetric quantification of antibiotic drug concentration
693   in bacterial cells for the characterization of translocation across bacterial
694   membranes. *Nature Protocols* **13**, 1348–1361 (2018).

695   47. Allam, A. *et al.* Microspectrofluorimetry to dissect the permeation of ceftazidime in
696   Gram-negative bacteria. *Sci Rep* **7**, (2017).

697   48. Andersen, C., Jordy, M. & Benz, R. Evaluation of the rate constants of sugar
698   transport through maltoporin (LamB) of *Escherichia coli* from the sugar-induced
699   current noise. *J Gen Physiol* **105**, 385–401 (1995).

700   49. Kullman, L., Winterhalter, M. & Bezrukov, S. M. Transport of maltodextrins
701   through maltoporin: a single-channel study. *Biophys J* **82**, 803–812 (2002).

702   50. Gutsmann, T., Heimburg, T., Keyser, U., Mahendran, K. R. & Winterhalter, M.
703   Protein reconstitution into freestanding planar lipid membranes for
704   electrophysiological characterization. *Nature Protocols* **10**, 188–198 (2015).

51. Mahendran, K. R., Kreir, M., Weingart, H., Fertig, N. & Winterhalter, M. Permeation of antibiotics through *Escherichia coli* OmpF and OmpC porins: Screening for influx on a single-molecule level. *J Biomol Screen* **15**, 302–307 (2010).

52. Mahendran, K. R. *et al.* Molecular basis of enrofloxacin translocation through OmpF, an outer membrane channel of *Escherichia coli* - When binding does not imply translocation. *J. Phys. Chem. B* **114**, 5170–5179 (2010).

53. Singh, P. R., Ceccarelli, M., Lovelle, M., Winterhalter, M. & Mahendran, K. R. Antibiotic permeation across the OmpF channel: Modulation of the affinity site in the presence of magnesium. *Journal of Physical Chemistry B* **116**, 4433–4438 (2012).

54. Wang, J., Bafna, J. A., Bhamidimarri, S. P. & Winterhalter, M. Small-molecule permeation across membrane channels: Chemical modification to quantify transport across OmpF. *Angewandte Chemie International Edition* **58**, 4737–4741 (2019).

55. Ghai, I. *et al.* Ampicillin permeation across OmpF, the major outer-membrane channel in *Escherichia coli*. *J. Biol. Chem.* **293**, 7030–7037 (2018).

56. Ghai, I. *et al.* General method to determine the flux of charged molecules through nanopores applied to β-lactamase inhibitors and OmpF. *J. Phys. Chem. Lett.* **8**, 1295–1301 (2017).

57. Winterhalter, M. & Ceccarelli, M. Physical methods to quantify small antibiotic molecules uptake into Gram-negative bacteria. *European Journal of Pharmaceutics and Biopharmaceutics* **95**, 63–67 (2015).

58. Scorciapino, M. A. *et al.* Rationalizing the permeation of polar antibiotics into Gram-negative bacteria. *J. Phys.: Condens. Matter* **29**, 113001 (2017).

59. Tieleman, D. P. & Berendsen, H. J. A molecular dynamics study of the pores formed by *Escherichia coli* OmpF porin in a fully hydrated palmitoyloleoylphosphatidylcholine bilayer. *Biophys J* **74**, 2786–2801 (1998).

60. Im, W. & Roux, B. Ion permeation and selectivity of OmpF porin: A theoretical study based on molecular dynamics, brownian dynamics, and continuum electrodiffusion theory. *Journal of Molecular Biology* **322**, 851–869 (2002).

736   61. Aguilella-Arzo, M., García-Celma, J. J., Cervera, J., Alcaraz, A. & Aguilella, V. M.
737   Electrostatic properties and macroscopic electrodiffusion in OmpF porin and
738   mutants. *Bioelectrochemistry* **70**, 320–327 (2007).
739   62. Biró, I., Pezeshki, S., Weingart, H., Winterhalter, M. & Kleinekathöfer, U.
740   Comparing the temperature-dependent conductance of the two structurally similar
741   *E. coli* porins OmpC and OmpF. *Biophysical Journal* **98**, 1830–1839 (2010).
742   63. Tran, Q.-T., Williams, S., Farid, R., Erdemli, G. & Pearlstein, R. The translocation
743   kinetics of antibiotics through porin OmpC: Insights from structure-based
744   solvation mapping using WaterMap. *Proteins: Structure, Function, and*
745   *Bioinformatics* **81**, 291–299 (2013).
746   64. Ceccarelli, M., Danelon, C., Laio, A. & Parrinello, M. Microscopic mechanism of
747   antibiotics translocation through a porin. *Biophysical Journal* **87**, 58–64 (2004).
748   65. Masi, M., Pagès, J.-M. & Winterhalter, M. Outer membrane porins. in *Bacterial*
749   *Cell Walls and Membranes* 1–54 (A. Kuhn, 2019).
750   66. Acosta-Gutierrez, S., Scorciapino, M. A., Bodrenko, I. & Ceccarelli, M. Filtering
751   with electric field: The case of *E. coli* porins. *J. Phys. Chem. Lett.* **6**, 1807–1812
752   (2015).
753   67. Bajaj, H. *et al.* Molecular basis of filtering carbapenems by porins from β-lactam-
754   resistant clinical strains of *Escherichia coli*. *J. Biol. Chem.* **291**, 2837–2847
755   (2016).
756   68. Acosta-Gutierrez, S., Bodrenko, I., Scorciapino, M. A. & Ceccarelli, M.
757   Macroscopic electric field inside water-filled biological nanopores. *Phys. Chem.*
758   *Chem. Phys.* **18**, 8855–8864 (2016).
759   69. Kojima, S. & Nikaido, H. High salt concentrations increase permeability through
760   OmpC channels of *Escherichia coli*. *J. Biol. Chem.* **289**, 26464–26473 (2014).
761   70. D'Agostino, T., Salis, S. & Ceccarelli, M. A kinetic model for molecular diffusion
762   through pores. *Biochimica et Biophysica Acta (BBA) - Biomembranes* **1858**,
763   1772–1777 (2016).
764   71. Bodrenko, I., Bajaj, H., Ruggerone, P., Winterhalter, M. & Ceccarelli, M. Analysis
765   of fast channel blockage: revealing substrate binding in the microsecond range.
766   *Analyst* **140**, 4820–4827 (2015).

767 72. Bodrenko, I. V., Wang, J., Salis, S., Winterhalter, M. & Ceccarelli, M. Sensing
768   single molecule penetration into nanopores: Pushing the time resolution to the
769   diffusion limit. *ACS Sens* **2**, 1184–1190 (2017).

770 73. Bajaj, H. *et al.* Bacterial outer membrane porins as electrostatic nanosieves:
771   Exploring transport rules of small polar molecules. *ACS Nano* **11**, 5465–5473
772   (2017).

773 74. Payne, D. J., Gwynn, M. N., Holmes, D. J. & Pompliano, D. L. Drugs for bad
774   bugs: confronting the challenges of antibacterial discovery. *Nature Reviews Drug
775   Discovery* **6**, 29–40 (2007).

776 75. O'Shea, R. & Moser, H. E. Physicochemical properties of antibacterial
777   compounds: Implications for drug discovery. *J. Med. Chem.* **51**, 2871–2878
778   (2008).

779 76. Brown, D. G., May-Dracka, T. L., Gagnon, M. M. & Tommasi, R. Trends and
780   exceptions of physical properties on antibacterial activity for Gram-positive and
781   Gram-negative pathogens. *J. Med. Chem.* **57**, 10144–10161 (2014).

782 77. Page, M. G. P. Beta-lactam antibiotics. in *Antibiotic Discovery and Development*
783   79–117 (Dougherty, T. J., and Pucci, M., Eds., 2011).

784 78. Bodrenko, I. V., Salis, S., Acosta-Gutierrez, S. & Ceccarelli, M. Diffusion of large
785   particles through small pores: from entropic to enthalpic transport. *J. Chem. Phys.*
786   **150**, 211102–211106 (2019).

787 79. Grabowicz, M. & Silhavy, T. J. Envelope stress responses: An interconnected
788   safety net. *Trends Biochem Sci* **42**, 232–242 (2017).

789 80. Chen, H. D. & Groisman, E. A. The biology of the PmrA/PmrB two-component
790   system: The major regulator of lipopolysaccharide modifications. *Annual Review
791   of Microbiology* **67**, 83–112 (2013).

792 81. Guest, R. L. & Raivio, T. L. Role of the Gram-negative envelope stress response
793   in the presence of antimicrobial agents. *Trends in Microbiology* **24**, 377–390
794   (2016).

795 82. Zschiedrich, C. P., Keidel, V. & Szurmant, H. Molecular mechanisms of two-
796   component signal transduction. *J Mol Biol* **428**, 3752–3775 (2016).

797 83. Laloux, G. & Collet, J.-F. Major Tom to ground control: How lipoproteins
798   communicate extracytoplasmic stress to the decision center of the cell. *J
799   Bacteriol* **199**, (2017).

800 84. Tiwari, S. *et al.* Two-component signal transduction systems of pathogenic
801   bacteria as targets for antimicrobial therapy: An overview. *Front Microbiol* **8**,
802   (2017).
803 85. Fröhlich, K. S. & Gottesman, S. Small regulatory RNAs in the enterobacterial
804   response to envelope damage and oxidative stress. *Microbiology Spectrum* **6**,
805   (2018).
806 86. Barquist, L. & Vogel, J. Accelerating discovery and functional analysis of small
807   RNAs with new technologies. *Annual Review of Genetics* **49**, 367–394 (2015).
808 87. Vogel, J. & Wagner, E. G. H. Target identification of small noncoding RNAs in
809   bacteria. *Current Opinion in Microbiology* **10**, 262–270 (2007).
810 88. Guillier, M., Gottesman, S. & Storz, G. Modulating the outer membrane with small
811   RNAs. *Genes Dev.* **20**, 2338–2348 (2006).
812 89. Vogel, J. & Papenfort, K. Small non-coding RNAs and the bacterial outer
813   membrane. *Current Opinion in Microbiology* **9**, 605–611 (2006).
814 90. Valentin-Hansen, P., Johansen, J. & Rasmussen, A. A. Small RNAs controlling
815   outer membrane porins. *Current Opinion in Microbiology* **10**, 152–155 (2007).
816 91. Delihas, N. & Forst, S. MicF: an antisense RNA gene involved in response of
817   *Escherichia coli* to global stress factors. *Journal of Molecular Biology* **313**, 1–12
818   (2001).
819 92. Andersen, J. & Delihas, N. *micF* RNA binds to the 5' end of *ompF* mRNA and to a
820   protein from *Escherichia coli. Biochemistry* **29**, 9249–9256 (1990).
821 93. Delihas, N. Discovery and characterization of the first non-coding RNA that
822   regulates gene expression, *micF* RNA: A historical perspective. *World J Biol*
823   *Chem* **6**, 272–280 (2015).
824 94. Inouye, M. The first demonstration of RNA interference to inhibit mRNA function.
825   *Gene* **592**, 332–333 (2016).
826 95. Ramani, N., Hedeshian, M. & Freundlich, M. *micF* antisense RNA has a major
827   role in osmoregulation of OmpF in *Escherichia coli. J Bacteriol* **176**, 5005–5010
828   (1994).
829 96. Chou, J. H., Greenberg, J. T. & Demple, B. Posttranscriptional repression of
830   *Escherichia coli* OmpF protein in response to redox stress: positive control of the
831   *micF* antisense RNA by the *soxRS* locus. *J Bacteriol* **175**, 1026–1031 (1993).

832   97. Chen, S., Zhang, A., Blyn, L. B. & Storz, G. MicC, a second small-RNA regulator
833   of Omp protein expression in *Escherichia coli*. *J Bacteriol* **186**, 6689–6697
834   (2004).
835   98. Dam, S., Pagès, J.-M. & Masi, M. Dual regulation of the small RNA MicC and the
836   quiescent porin OmpN in response to antibiotic stress in *Escherichia coli*.
837   *Antibiotics (Basel)* **6**, (2017).
838   99. Blair, J. M. A., Webber, M. A., Baylay, A. J., Ogbolu, D. O. & Piddock, L. J. V.
839   Molecular mechanisms of antibiotic resistance. *Nat. Rev. Microbiol.* **13**, 42–51
840   (2015).
841   100.   Du, D. *et al.* Multidrug efflux pumps: structure, function and regulation. *Nature*
842   *Reviews Microbiology* **16**, 523 (2018).
843   101.   Davin-Regli, A. *et al.* Membrane permeability and regulation of drug "influx and
844   efflux" in enterobacterial pathogens. *Curr Drug Targets* **9**, 750–759 (2008).
845   102.   Dupont, H. *et al.* Structural alteration of OmpR as a source of ertapenem
846   resistance in a CTX-M-15-producing *Escherichia coli* O25b:H4 sequence type
847   131 clinical isolate. *Antimicrobial Agents and Chemotherapy* **61**, e00014-17
848   (2017).
849   103.   Dupont, H. *et al.* Molecular characterization of carbapenem-nonsusceptible
850   enterobacterial isolates collected during a prospective interregional survey in
851   France and susceptibility to the novel ceftazidime-avibactam and aztreonam-
852   avibactam combinations. *Antimicrobial Agents and Chemotherapy* **60**, 215–221
853   (2016).
854   104.   Tran, Q.-T. *et al.* Implication of porins in β-lactam resistance of *Providencia*
855   *stuartii*. *J Biol Chem* **285**, 32273–32281 (2010).
856   105.   Tran, Q.-T. *et al.* Porin flexibility in *Providencia stuartii*: cell-surface-exposed
857   loops L5 and L7 are markers of *Providencia* porin OmpPst1. *Research in*
858   *Microbiology* **168**, 685–699 (2017).
859   106.   Oteo, J. *et al.* Emergence of imipenem resistance in clinical *Escherichia coli*
860   during therapy. *International Journal of Antimicrobial Agents* **32**, 534–537 (2008).
861   107.   Philippe, N. *et al. In vivo* evolution of bacterial resistance in two cases of
862   *Enterobacter aerogenes* infections during treatment with imipenem. *PLoS One*
863   **10**, (2015).

864 108. Lázaro-Perona, F. *et al.* Genomic path to pandrug resistance in a clinical
865   isolate of *Klebsiella pneumoniae*. *International Journal of Antimicrobial Agents* **52**,
866   713–718 (2018).

867 109. Yang, F.-C., Yan, J.-J., Hung, K.-H. & Wu, J.-J. Characterization of
868   ertapenem-resistant *Enterobacter cloacae* in a Taiwanese University Hospital. *J*
869   *Clin Microbiol* **50**, 223–226 (2012).

870 110. Fernández, J., Guerra, B. & Rodicio, M. R. Resistance to carbapenems in non-
871   typhoidal *Salmonella enterica* Serovars from humans, animals and food. *Vet Sci*
872   **5**, (2018).

873 111. Doumith, M., Ellington, M. J., Livermore, D. M. & Woodford, N. Molecular
874   mechanisms disrupting porin expression in ertapenem-resistant *Klebsiella* and
875   *Enterobacter* spp. clinical isolates from the UK. *J. Antimicrob. Chemother.* **63**,
876   659–667 (2009).

877 112. Wozniak, A. *et al.* Porin alterations present in non-carbapenemase-producing
878   *Enterobacteriaceae* with high and intermediate levels of carbapenem resistance
879   in Chile. *Journal of Medical Microbiology* **61**, 1270–1279 (2012).

880 113. Cerqueira, G. C. *et al.* Multi-institute analysis of carbapenem resistance
881   reveals remarkable diversity, unexplained mechanisms, and limited clonal
882   outbreaks. *Proc Natl Acad Sci U S A* **114**, 1135–1140 (2017).

883 114. Novais, Â. *et al.* Spread of an OmpK36-modified ST15 *Klebsiella pneumoniae*
884   variant during an outbreak involving multiple carbapenem-resistant
885   *Enterobacteriaceae* species and clones. *Eur J Clin Microbiol Infect Dis* **31**, 3057–
886   3063 (2012).

887 115. Shin, S. Y. *et al.* Resistance to carbapenems in sequence type 11 *Klebsiella*
888   *pneumoniae* is related to DHA-1 and loss of OmpK35 and/or OmpK36. *Journal of*
889   *Medical Microbiology* **61**, 239–245 (2012).

890 116. Martínez-Martínez, L. Extended-spectrum beta-lactamases and the
891   permeability barrier. *Clin. Microbiol. Infect.* **14 Suppl 1**, 82–89 (2008).

892 117. Thiolas, A., Bollet, C., Scola, B. L., Raoult, D. & Pagès, J.-M. Successive
893   emergence of *Enterobacter aerogenes* strains resistant to imipenem and colistin
894   in a patient. *Antimicrobial Agents and Chemotherapy* **49**, 1354–1358 (2005).

895 118. Lavigne, J.-P. *et al.* An adaptive response of *Enterobacter aerogenes* to
896   imipenem: regulation of porin balance in clinical isolates. *International Journal of*
897   *Antimicrobial Agents* **41**, 130–136 (2013).

898 119. Lavigne, J.-P. *et al.* Membrane permeability, a pivotal function involved in
899   antibiotic resistance and virulence in *Enterobacter aerogenes* clinical isolates.
900   *Clinical Microbiology and Infection* **18**, 539–545 (2012).
901 120. Hamzaoui, Z. *et al.* An outbreak of NDM-1-producing *Klebsiella pneumoniae*,
902   associated with OmpK35 and OmpK36 porin loss in Tunisia. *Microbial Drug*
903   *Resistance* **24**, 1137–1147 (2018).
904 121. Gröbner, S. *et al.* Emergence of carbapenem-non-susceptible extended-
905   spectrum β-lactamase-producing *Klebsiella pneumoniae* isolates at the university
906   hospital of Tübingen, Germany. *Journal of Medical Microbiology* **58**, 912–922
907   (2009).
908 122. Findlay, J., Hamouda, A., Dancer, S. J. & Amyes, S. G. B. Rapid acquisition of
909   decreased carbapenem susceptibility in a strain of *Klebsiella pneumoniae* arising
910   during meropenem therapy. *Clinical Microbiology and Infection* **18**, 140–146
911   (2012).
912 123. Knopp, M. & Andersson, D. I. Amelioration of the fitness costs of antibiotic
913   resistance due to reduced outer membrane permeability by upregulation of
914   alternative porins. *Mol Biol Evol* **32**, 3252–3263 (2015).
915 124. Nelson, K. *et al.* Resistance to ceftazidime-avibactam is due to transposition of
916   KPC in a porin-deficient strain of *Klebsiella pneumoniae* with increased efflux
917   activity. *Antimicrobial Agents and Chemotherapy* **61**, e00989-17 (2017).
918 125. Shen, Z. *et al.* High ceftazidime hydrolysis activity and porin OmpK35
919   deficiency contribute to the decreased susceptibility to ceftazidime/avibactam in
920   KPC-producing *Klebsiella pneumoniae*. *J Antimicrob Chemother* **72**, 1930–1936
921   (2017).
922 126. Pagès, J.-M., Peslier, S., Keating, T. A., Lavigne, J.-P. & Nichols, W. W. Role
923   of the outer membrane and porins in susceptibility of β-lactamase-producing
924   *Enterobacteriaceae* to ceftazidime-avibactam. *Antimicrob. Agents Chemother.* **60**,
925   1349–1359 (2016).
926 127. Balabanian, G., Rose, M., Manning, N., Landman, D. & Quale, J. Effect of
927   porins and *bla*$_{KPC}$ expression on activity of imipenem with relebactam in *Klebsiella*
928   *pneumoniae*: Can antibiotic combinations overcome resistance? *Microbial Drug*
929   *Resistance* **24**, 877–881 (2018).

128. Sun, D., Rubio-Aparicio, D., Nelson, K., Dudley, M. N. & Lomovskaya, O. Meropenem-vaborbactam resistance selection, resistance prevention, and molecular mechanisms in mutants of KPC-producing *Klebsiella pneumoniae*. *Antimicrob. Agents Chemother.* **61**, (2017).

129. Lunha, K. *et al.* High-level carbapenem-resistant OXA-48-producing *Klebsiella pneumoniae* with a novel OmpK36 variant and low-level, carbapenem-resistant, non-porin-deficient, OXA-181-producing *Escherichia coli* from Thailand. *Diagnostic Microbiology and Infectious Disease* **85**, 221–226 (2016).

130. Dé, E. *et al.* A new mechanism of antibiotic resistance in *Enterobacteriaceae* induced by a structural modification of the major porin. *Molecular Microbiology* **41**, 189–198 (2001).

131. Thiolas, A., Bornet, C., Davin-Régli, A., Pagès, J.-M. & Bollet, C. Resistance to imipenem, cefepime, and cefpirome associated with mutation in Omp36 osmoporin of *Enterobacter aerogenes*. *Biochemical and Biophysical Research Communications* **317**, 851–856 (2004).

132. García-Fernández, A. *et al.* An ertapenem-resistant extended-spectrum-β-lactamase-producing *Klebsiella pneumoniae* clone carries a novel OmpK36 porin variant. *Antimicrobial Agents and Chemotherapy* **54**, 4178–4184 (2010).

133. Clancy, C. J. *et al.* Mutations of the ompK36 porin gene and promoter impact responses of sequence type 258, KPC-2-producing *Klebsiella pneumoniae* strains to doripenem and doripenem-colistin. *Antimicrob Agents Chemother* **57**, 5258–5265 (2013).

134. Papagiannitsis, C. C. *et al.* OmpK35 and OmpK36 porin variants associated with specific sequence types of *Klebsiella pneumoniae*. *Journal of Chemotherapy* **25**, 250–254 (2013).

135. Hall, J. M., Corea, E., Sanjeewani, H. D. A. & Inglis, T. J. J. Molecular mechanisms of β-lactam resistance in carbapenemase-producing *Klebsiella pneumoniae* from Sri Lanka. *Journal of Medical Microbiology* **63**, 1087–1092 (2014).

136. Partridge, S. R. *et al.* Emergence of *bla*KPC carbapenemase genes in Australia. *International Journal of Antimicrobial Agents* **45**, 130–136 (2015).

961   137.   García-Sureda, L. *et al.* OmpK26, a novel porin associated with carbapenem
962   resistance in *Klebsiella pneumoniae*. *Antimicrob Agents Chemother* **55**, 4742–
963   4747 (2011).

964   138.   Bialek-Davenet, S. *et al. In-vivo* loss of carbapenem resistance by extensively
965   drug-resistant *Klebsiella pneumoniae* during treatment via porin expression
966   modification. *Sci Rep* **7**, (2017).

967   139.   Kaczmarek, F. M., Dib-Hajj, F., Shang, W. & Gootz, T. D. High-level
968   carbapenem resistance in a *Klebsiella pneumoniae* clinical isolate is due to the
969   combination of bla_{ACT-1} β-lactamase production, porin OmpK35/36 insertional
970   inactivation, and down-regulation of the phosphate transport porin PhoE.
971   *Antimicrobial Agents and Chemotherapy* **50**, 3396–3406 (2006).

972   140.   Doménech-Sánchez, A., Hernández-Allés, S., Martínez-Martínez, L., Benedí,
973   V. J. & Albertí, S. Identification and characterization of a new porin gene of
974   *Klebsiella pneumoniae*: Its role in β-lactam antibiotic resistance. *J Bacteriol* **181**,
975   2726–2732 (1999).

976   141.   Castanheira, M., Mendes, R. E. & Sader, H. S. Low frequency of ceftazidime-
977   avibactam resistance among *Enterobacteriaceae* isolates carrying bla_{KPC}
978   collected in U.S. hospitals from 2012 to 2015. *Antimicrob Agents Chemother* **61**,
979   (2017).

980   142.   Noinaj, N., Gumbart, J. C. & Buchanan, S. K. The β-barrel assembly
981   machinery in motion. *Nat Rev Microbiol* **15**, 197–204 (2017).

982   143.   Schiffrin, B., Brockwell, D. J. & Radford, S. E. Outer membrane protein folding
983   from an energy landscape perspective. *BMC Biol* **15**, (2017).

984   144.   Robinson, J. A. Folded synthetic peptides and other molecules targeting outer
985   membrane protein complexes in Gram-negative bacteria. *Front Chem* **7**, (2019).

986   145.   Hao, M. *et al.* Porin deficiency in carbapenem-resistant *Enterobacter*
987   *aerogenes* strains. *Microbial Drug Resistance* **24**, 1277–1283 (2018).

988   146.   Jiménez-Castellanos, J.-C. *et al.* Envelope proteome changes driven by RamA
989   overproduction in *Klebsiella pneumoniae* that enhance acquired β-lactam
990   resistance. *J. Antimicrob. Chemother.* **73**, 88–94 (2018).

991   147. Chetri, S. *et al.* Transcriptional response of OmpC and OmpF in *Escherichia*
992   *coli* against differential gradient of carbapenem stress. *BMC Research Notes* **12**,
993   138 (2019).
994

995   **BOXES REFERENCES**

996   148. Bhamidimarri, S. P., Prajapati, J. D., van den Berg, B., Winterhalter, M. &
997   Kleinekathöfer, U. Role of electroosmosis in the permeation of neutral molecules:
998   CymA and cyclodextrin as an example. *Biophys J* **110**, 600–611 (2016).

999   149. Talbot, G. H. β-Lactam antimicrobials: what have you done for me lately?
1000   *Annals of the New York Academy of Sciences* **1277**, 76–83 (2013).

1001   150. Olivares, J. *et al.* The intrinsic resistome of bacterial pathogens. *Front*
1002   *Microbiol* **4**, (2013).

1003   151. Li, X.-Z., Plésiat, P. & Nikaido, H. The challenge of efflux-mediated antibiotic
1004   resistance in Gram-negative bacteria. *Clin Microbiol Rev* **28**, 337–418 (2015).

1005   152. Xia, J., Gao, J. & Tang, W. Nosocomial infection and its molecular
1006   mechanisms of antibiotic resistance. *BioScience Trends* **10**, 14–21 (2016).

1007   153. Nikaido, H. & Pagès, J.-M. Broad specificity efflux pumps and their role in
1008   multidrug resistance of Gram negative bacteria. *FEMS Microbiol Rev* **36**, 340–
1009   363 (2012).

1010   154. Davin-Regli, A., Lavigne, J.-P. & Pagès, J.-M. *Enterobacter* spp.: Update on
1011   taxonomy, clinical aspects, and emerging antimicrobial resistance. *Clinical*
1012   *Microbiology Reviews* **32**, e00002-19 (2019).

1013   155. Pagès, J.-M. *et al.* Efflux Pump, the masked side of ß-Lactam resistance in
1014   *Klebsiella pneumoniae* clinical isolates. *PLOS ONE* **4**, e4817 (2009).

1015   156. Westfall, D. A. *et al.* Bifurcation kinetics of drug uptake by Gram-negative
1016   bacteria. *PLOS ONE* **12**, e0184671 (2017).

1017   157. Nicolas-Chanoine, M.-H., Mayer, N., Guyot, K., Dumont, E. & Pagès, J.-M.
1018   Interplay between membrane permeability and enzymatic barrier leads to
1019   antibiotic-dependent resistance in *Klebsiella pneumoniae. Front Microbiol* **9**,
1020   (2018).

1021   158. Wan Nur Ismah, W. A. K., Takebayashi, Y., Findlay, J., Heesom, K. J. &
1022   Avison, M. B. Impact of OqxR loss of function on the envelope proteome of

1023 *Klebsiella pneumoniae* and susceptibility to antimicrobials. *J Antimicrob*
1024 *Chemother* **73**, 2990–2996 (2018).

1025 159. Castanheira, M. *et al.* Analyses of a ceftazidime-avibactam-resistant
1026 *Citrobacter freundii* isolate carrying *bla*KPC-2 reveals a heterogenous population
1027 and reversible genotype. *mSphere* **3**, (2018).

1028 160. Fajardo-Lubián, A., Ben Zakour, N. L., Agyekum, A., Qi, Q. & Iredell, J. R.
1029 Host adaptation and convergent evolution increases antibiotic resistance without
1030 loss of virulence in a major human pathogen. *PLoS Pathog* **15**, (2019).

1031 161. Nikaido, H. Role of permeability barriers in resistance to β-lactam antibiotics.
1032 *Pharmacology & Therapeutics* **27**, 197–231 (1985).

1033

1034 **FIGURES REFERENCE**

1035
1036 162 Coines, J., Acosta-Gutierrez, S., Bodrenko, I., Rovira, C. & Ceccarelli, M.
1037 Glucose transport via the pseudomonads porin OprB. Implications for the design
1038 of Trojan-horse antinfectives. *Phys. Chem. Chem. Phys.* **21**, 8457–8463 (2019).

1039

FIGURE LEGENDS

Figure 1: Structural aspects of enterobacterial porins

Extracellular (**a**) and side views (**b**) of the OmpC trimer, with L2 coloured green and the pore-constricting loop L3 coloured magenta. Loops have been smoothened for clarity. OM, outer membrane. **c, d** Extracellular (**c**) and slabbed side views (**d**) of an OmpC monomer with the residues lining the eyelet of the constriction region (CR) shown by stick models. **e,** Cross-section through OmpC showing the internal funnel-like shape of the channel coloured by electrostatic potential. The constriction region (CR) is indicated. **f,** View as in **e**, but close-up and with residues on both sides of the CR shown as stick models.

Figure 2: Structural differences in enterobacterial porins have implications for permeation and antibiotic resistance.

Superposed cartoon views for OmpC orthologs from *E. coli* (**a**), *K. pneumoniae* (**b**) and *E. aerogenes* (**c**). The bottom row shows the corresponding OmpF orthologs (**d-f**). The eyelet-lining residues equivalent to K16, R37, R74, R124, D105 and E109 of *E. coli* OmpC are shown as grey stick models. These key residues are identical in Enterobacterial porins. Examples of equivalent residues near the constriction zone that differ between OmpC and OmpF proteins are labeled and shown as yellow stick models (*e.g.* Q33, W72, G116 and K317 in *E. coli* OmpC, M38, K80, Y124 and I314 in *E. coli* OmpF). Subtle differences in structure such as these can lead to alteration of the electric field close to and within the constriction zone, which in turn can result in a decreased translocation efficacy of antibiotic across the channel, thus contributing to the emergence of resistance.

Figure 3: Mechanism of translocation/Permeation model of molecules through general porins.

The translocation of the zwitterionic meropenem through OmpF. Shown in red surface are the acidic residues of loop L3 and in blue surface the residues of the basic ladder. Loop L3 is shown in magenta. The colored spheres indicate the carboxylic and the amine group (pyrrolidine) of meropenem, respectively in red and blue. The colored arrows represent the electric dipole moment of meropenem.

Recent results suggest a free energy landscape model for the passive diffusion of molecules through porins from *Enterobacteriaceae*, as depicted in the figure. The downward diffusion of meropenem in the constriction region, highlighted as a rectangular box, starts by (arrow orange) attraction of the carboxylic group towards the residues R167-R168; (arrow pink) alignment of the dipole to the transversal electric field in the preorientation region with the amine group pointing toward the loop L3; (arrow yellow) sliding of the meropenem in the CR maintaining the dipole aligned with the transversal electric field, with the carboxylic group along the basic ladder and the amine group pointing the loop L3; (arrow green) exit of the meropenem from the CR by rotation of the dipole[66]. Since the porins are characterized by an hourglass shape, a steric barrier will be always present (black energy profile), strongly limiting the permeability. In order to increase the flux an electrostatic compensation of the barrier is needed[58] (orange dotted energy profile), which occurs when the dipole moment of the molecule aligns with the transversal electric field inside the pore (yellow arrow of meropenem). On the other hand, if the electrostatic interactions create a strong binding site as in substrate-specific channels, as it may happen in the preorientation region[33] (pink arrow), the pore might reach saturation and the increase of the flux would be limited at high concentration[162]. In the limit of low concentration, the flux at concentration gradient ΔC is quantified in terms of the permeability coefficient through a single pore P, calculated knowing the potential of mean force $F(z)$ (molecule-pore-water interaction) and the diffusion constant of the molecule inside the pore $D(z)$. Only when considering the complete interaction of the molecule inside the entire pore (to note the integral over the pore length L) it would be possible to predict the flux. This explains why early efforts using docking methods, via searching for local affinity/binding sites, failed to provide guidance rules for transport.

Commented [LM9]: And F(0) definition ?

Commented [MC10]: F(0) is the energy at the entry of the pore, I added it in the new Fig.3 as the indication of z-axis

BOX 1: Counting permeating molecules with an exit barrier.

a

b
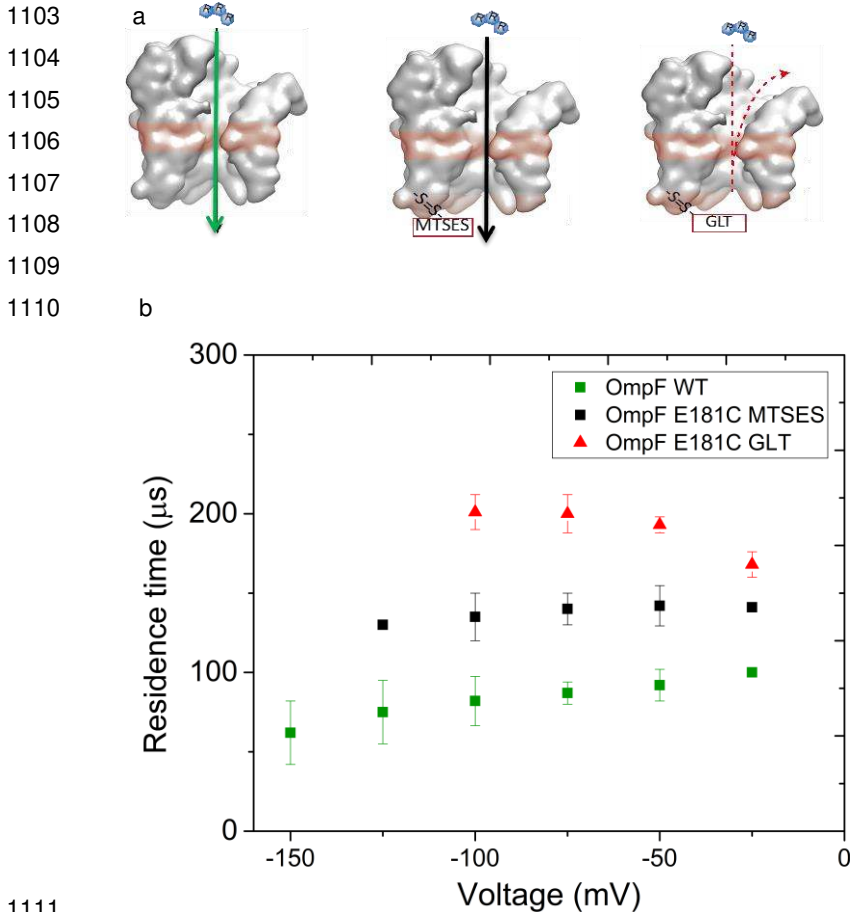
Information on the contribution of the individual porin on permeation can be obtained via single channel reconstitution into planar lipid bilayer. The molecule needs to enter the channel and block the ion current sufficiently. To distinguish binding from translocation we apply external forces pushing or pulling the molecule while recording their residence time. For charged molecule we may use electric fields[54,148]. In the case of uncharged molecules, electro-osmosis can be considered[148]. The latter effect originates from excess of charged residues in the constriction zone: porins often are cation selective, which typically implies an excess of negatively charged residues at the channel surface combined with a cloud of mobile cationic

1122 counterions. Application of an external voltage will cause a flow of the counterions
1123 along the field creating a net flow pushing molecules. Surprisingly this effect is quite
1124 strong and comparable to diffusion already at μM concentration gradient.

1125 As an example to detect fast permeating molecules or to distinguish molecules which
1126 permeate from those which only binds and reflects backwards, a barrier at the exit
1127 has been engineered. Above we show an example of OmpF from *E. coli*. A single
1128 point mutation in OmpF at position 181 OmpF^{E181C} was introduced and crosslinked
1129 with either the small blocker Sodium (2-sulfonatoethyl) MethaneThioSulfonate
1130 (MTSES) or the large blocker glutathione (see the figure 1). Tri-arginine is a charged
1131 molecule that is pulled into the channel under negative applied voltage. Tri-arginine
1132 permeates efficiently through OmpF (see lhs in figure a) and could not be detected
1133 previously, higher negative voltage leads to faster permeation (figure 1b, green
1134 squares). The modification of OmpF^{E181C} by MTSES creates a barrier at the exit that
1135 is sufficient to alter the pathway of Tri-arginine (Arg-Arg-Arg), on average the
1136 triargnine stays longer in the channel (figure 1b, black squares). In the case of GLT
1137 (figure 1a, rhs), the molecule has to return against the electric field leading to a
1138 pronounced residence time with increasing field strength (figure 1b, red triangles)[5].
1139 This approach might enable the discrimination of blockage events from translocation
1140 events for a wide range of substrates while working in the μM range. As the data
1141 analysis is straightforward, parallelisation of experiments might be possible. A
1142 potential application of this technique could include screening for molecular
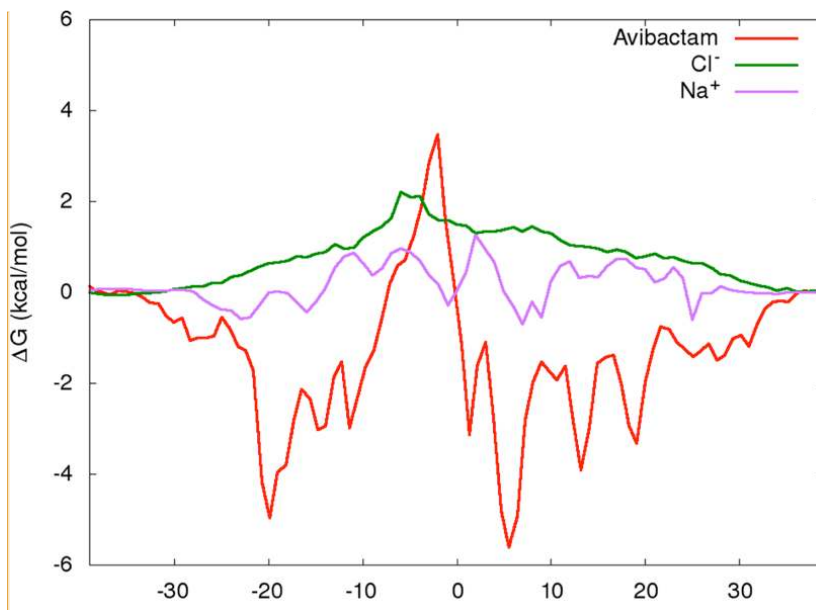1143 structures to improve the permeability of antibiotics.

1144
1145
1146

Commented [LM11]: Maybe I m missing something :Does MTSES really block or it's more difficult to permeate. I find the legend does not explain well the differences betweenthe two blockers.

1147 **BOX 2: Transport of charged compounds revealed by a concentration gradient.**

1148 Electrolyte solutions always contain an equal amount of charges. Application of a

1149 concentration gradient across the membrane results in a diffusion-driven flux. In most

1150 cases, one of the ions diffuses faster than the counter ion and the difference in flux

1151 creates a diffusion potential and provides information on the channel selectivity but

1152 not on the absolute flux. However, in combination with single channel conductance

1153 data it is possible to extract the true flux of the individual ions[56].

1154

Commented [LM12]: Need to be rephrased. Link between the two paragraphs of the box not clear. 'However, combination of single channel conductance data and molecular dynamics modelling provide information on the true flux of the individual ions '

Commented [LM13]: X axis missing: Z (A)

1155

1156 Computer modelling can nowadays predict the energy barrier of a molecule along the

1157 channel axis which allows to obtain an estimate for the flux. In the above figure we

1158 show the free-energy surface of avibactam along the Z axis of diffusion and, for a

1159 comparison with free energies of Cl−and Na+ ions, calculated using their relative

1160 densities with respect to the bulk. Note that OmpF is slightly cation selective and the

1161 preference for cations is reflected by a slight affinity. In contrast anions are exposed

1162 to a shallow energy barrier. Avibactam has a narrow but high barrier in the middle

1163 combined with two affinity sites before and after the barrier[56]. We expect that in the

1164 near future such energy profiles can be obtained in a semi-automated manner from

1165 larger libraries which later may be experimentally identified.

BOX 3: Interplay between porin alteration, ß-lactamase and efflux pump activities in internal concentration of active antibiotics.

It is now recognized that three key factors, - the outer membrane permeability, -the enzymatic degradation and - the efflux pumps, efficiently govern the internal concentration of active ß-lactams close to its periplasmic target.

Regarding the clinical isolates, these mechanisms acting alone or together drastically alter the antibacterial spectrum of the molecule alone or the combination ß-lactam + ß-lactamase inhibitor used during patient treatment. Some possible clinical events are illustrated in the following figure.

In medium column (**c,d,e,f,g**) the strains exhibit a normal porin expression, in contrast right column (**h,i,j,k,l**) represent a altered porin phenotype (lack or mutation of channel function). Several combinations are hypothesized in '**c**' to '**l**', for instance: in '**i**', porin alteration + ß-lactamase overexpression generating a decrease of ß-lactam susceptibility, or in '**l**' porin alteration + ß-lactamase overexpression + efflux conferring a total resistance. These well-combined strategies have been reported in numerous *Klebsiella* or *Enterobacter* isolates and they strongly impair ß-lactams activities. It is important to note that a reduced penetration (porin alteration) and/or an efflux activity strongly reinforce the effect of enzymatic barrier and, by side effect, contribute to the induction of ß-lactamase expression. This sophisticated management used by the bacterial genius of internal concentration of active ß-lactams contributes to bacterial survival and therapeutic failure. For reviews see [99,100,149-154] and some recent selected papers[126,138,146,155-160].

It must be noted that a fraction of the expelled antibiotics can re-enter bacterial cell (dashed brown arrows) for a second run in contrast to the ß-lactams treated by ß-lactamases that are cleaved (green arrows).
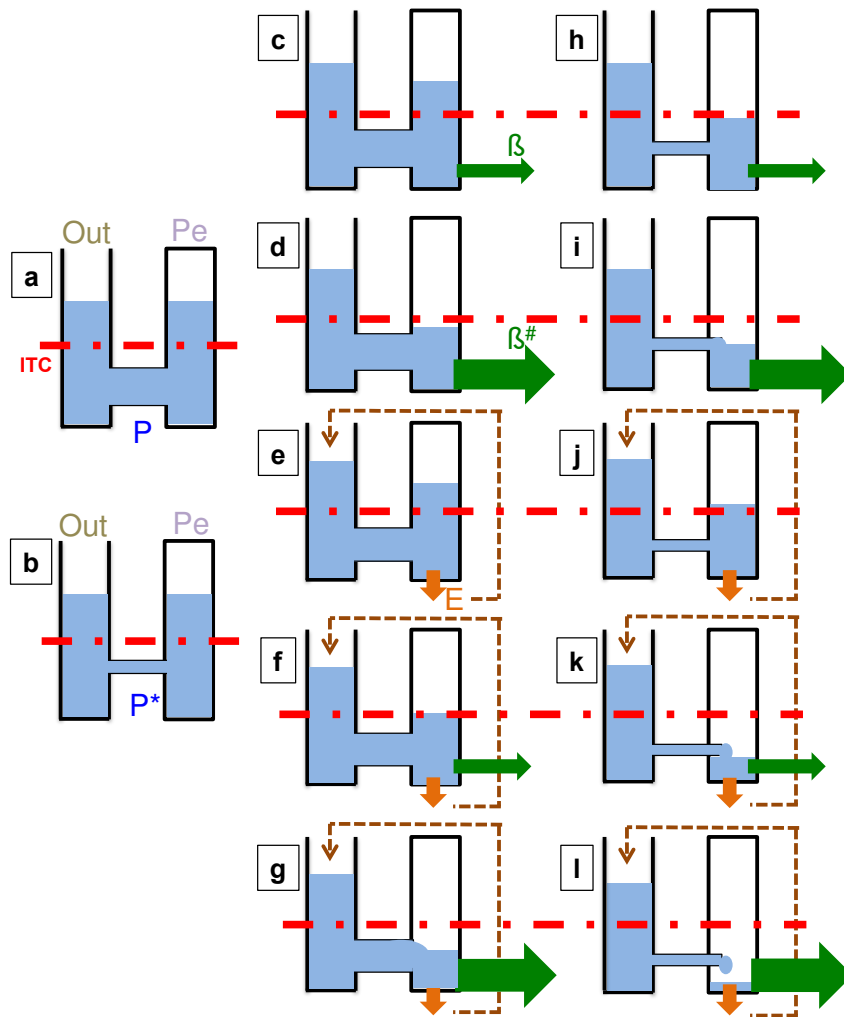
1194

1195

1196 **Legend:**

1197 The antibiotic flux across the porin, from external medium (left column, Out) to

1198 periplasmic space (right column, Pe), is illustrated by the channel joining the two

1199 compartments. The maximal diameter of the channel (P in **a**) represents the normal
1200 wild type porin production (number of copies, normal conductance), the small
1201 diameter (P* in **b**) corresponds to a porin alteration (diminution of porin expression, a
1202 change of porin type (OmpF > PhoE) or a mutation inducing an alteration of channel
1203 properties in CR for instance). For reviews see [5,65,99,100,138,150].

1204 ß indicates the presence of ß-lactamases that cleave ß-lactam molecules in
1205 periplasmic space decreasing the number of active antibiotics and ß[#] illustrates the
1206 overproduction of ß-lactamases (green arrows). E indicates the presence of active
1207 efflux pumps that expel the antibiotic outside the bacterial cell [6,17,146,150-155,158]. The
1208 antibiotic ejected by efflux pump (E) can re-enter bacterial cell (dashed brown
1209 arrows) for a second try.

1210 ITC (for internal threshold concentration, red dashed lane) represents the theoretical
1211 concentration necessary to inhibit the function of bacterial target. We have arbitrary
1212 fixed the alteration of penetration (due to mutation or porin lack), the rate of
1213 periplasmic hydrolysis and the effect of antibiotic efflux on internal antibiotic level.
1214 The resulting level of antibiotic accumulation is only roughly estimated to give a
1215 simple schema of the respective contributions of the three mechanisms.

1216 This figure is an upgrade of the pioneer H. Nikaido's model describing the interplay
1217 "porin-ß lactamase" in resistance[161].

1218